The effect of delocalization on the exchange energy in *meta*- and *para*-linked Pt-containing carbazole polymers and monomers

Ning Zhang and Anna Hayer
Cavendish Laboratory, University of Cambridge, Cambridge CB3 0HE, United Kingdom

Mohammed K. Al-Suti, Rayya A. Al-Belushi, and Muhammad S. Khan
Department of Chemistry, College of Science, Sultan Qaboos University, Al-Khodh 123, Sultanate of Oman

Anna Köhler[a)]
Cavendish Laboratory, University of Cambridge, Cambridge CB3 0HE, United Kingdom and Institute of Physics, University of Potsdam, 14469 Potsdam, Germany

(Received 9 May 2005; accepted 4 April 2006; published online 23 June 2006)

A series of novel platinum-containing carbazole monomers and polymers was synthesized and fully characterized by UV-VIS absorption, luminescence, and photoinduced absorption studies. In these compounds, a carbazole unit is incorporated into the main chain via either a *para*- or a *meta*-linkage. We discuss the effects of linkage and polymerization on the energy levels of S_1, T_1, and T_n. The S_1-T_1 splitting observed for the *meta*-linked monomer (0.4 eV) is only half of that in the *para*-linked monomer (0.8 eV). Upon polymerization, the exchange energy in the *para*-linked compound reduces, yet still remains larger than in the *meta*-linked polymer. We attribute the difference in exchange energy to the difference in wave function overlap between electron and hole in these compounds. © *2006 American Institute of Physics*. [DOI: 10.1063/1.2200351]

I. INTRODUCTION

In the past decade, great efforts have been devoted to the design and synthesis of light-emitting organic polymers in the scientific community because of their potential applications in optoelectronic devices such as light-emitting diodes (LEDs), lasers, and photocells.[1–3] During LED operation, a large fraction of triplet excitons may be formed[4–9] and high LED efficiencies have been demonstrated when such triplet excitons are transferred onto organometallic phosphorescent guest molecules.[10,11]

This triplet harvesting process requires host materials with a high triplet T_1 energy level, in particular, when green or blue phosphorescence is to be achieved. Yet at the same time, the singlet S_1 energy level should not be too high so that charge injection or transport via the highest occupied molecular orbital (HOMO) or lowest unoccupied molecular orbital (LUMO) levels is still feasible. Consequently, host materials should have a small S_1-T_1 energy gap, i.e., a low exchange energy. Unfortunately, in many rigid-rod polymers, the singlet S_1 energy level is about 0.7 eV above the triplet T_1 level due to a large overlap of electron and hole wave functions.[12,13]

Materials containing a carbazole unit are often used as host materials as some carbazole derivatives have a particularly small S_1-T_1 gap.[14–19] In a recent publication, Brunner *et al.* have shown that this gap can be as small as 0.45 eV in carbazole dimers and carbazole trimers[18] and yet becomes as large as 0.7–0.8 eV in mixed carbazole/fluorene oligomers. If carbazole is combined with fluorene, Brunner *et al.* suggest that the T_1 energy level is determined by the longest poly(*p*-phenylene) chain in the structure.

Here we have studied the effect that increased chain length has on the energy levels of the excited states and, in particular, on the exchange energy, when a conjugated polymer is connected via a *meta*-linkage or a *para*-linkage. We therefore compare materials where the carbazole unit is incorporated via 3,6 (*meta*) or 2,7 (*para*) positions into the platinum monomer and polymer as shown in Figs. 1(a) and 1(b). The effect of alkyl substitution at the 9 position was also studied. The comparison of analogous monomers and polymers allows us to establish the amount of delocalization that is achieved via the different linkages. The incorporation of platinum into the molecular backbone introduces strong spin-orbit coupling so that phosphorescence from the carbazole unit can be detected with ease. We find that firstly, polymerization reduces the exchange energy when the connection to the carbazole unit is made via a *para*-linkage, but that secondly, this exchange energy is higher in *para*- than in *meta*-connected systems.

II. EXPERIMENT

A. Synthetic procedures

All reactions were performed under a dry nitrogen atmosphere using standard Schlenk or glovebox techniques. All chemicals, except where stated otherwise, were obtained from Sigma Aldrich and used as received. Solvents were predried and distilled before use by standard procedures.[20]

[a)]Electronic mail: annak@rz.uni-potsdam.de

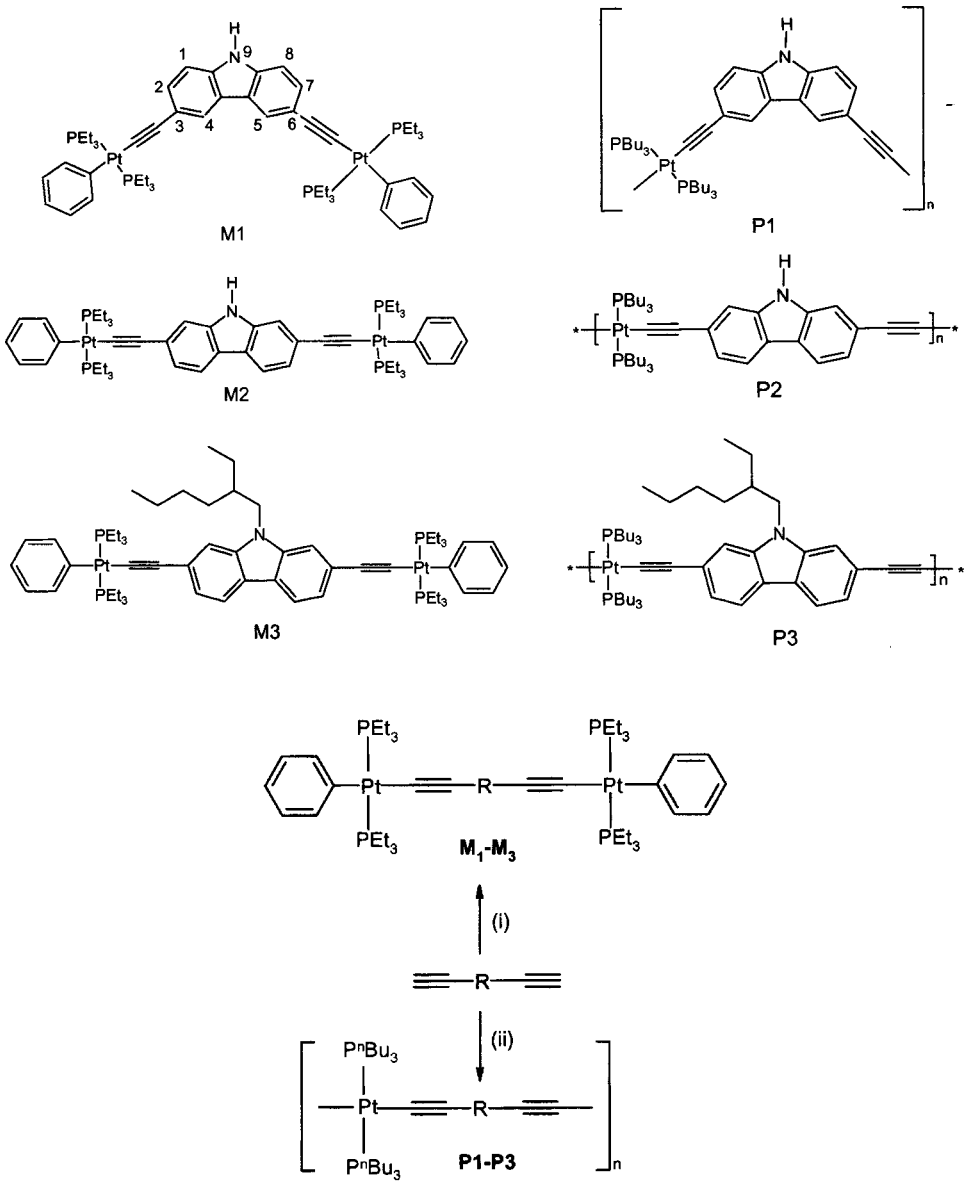

FIG. 1. (a) Chemical structures of the monomers M1, M2, and M3 and the polymers P1, P2, and P3. For M1 carbon atoms labels are also given. (b). Synthesis scheme of the Pt(II) diynes and poly-ynes.

The compounds *trans*-$[(Ph)(PEt_3)_2PtCl]$,[21] *trans*-$[(P^nBu_3)_2PtCl_2]$,[22] 3,6-diethynylcarbazole,[23,24] 2,7-diethynylcarbazole,[25] and *N*-octyl-2,7-diethynylcarbazole[25] were prepared by adaptation of literature procedures. Microanalyses were performed in the University Chemical Laboratory, University of Cambridge. IR spectra were recorded in CH_2Cl_2 solution in a NaCl cell on a Perkin-Elmer 1710 Fourier transform infrared (FTIR) spectrometer. The NMR spectra were recorded on a Bruker WM-250 or AM-400 spectrometer in $CDCl_3$ solvent. The ^1H and $^{13}C\{^1H\}$ NMR spectra were referenced to solvent resonances and $^{31}P\{^1H\}$ NMR spectra were referenced to external trimethylphosphite. Column chromatography was performed either on Kieselgel 60 (230–400 meshes) silica gel or alumina (Brockman grade II–III). Molar masses of the Pt(II) diynes were determined by fast atom bombardment (FAB) technique. For the Pt(II) poly-ynes, molar masses were determined by gel permeation chromatography (GPC) method,[26] using two PL Gel 30 cm, 5 μm mixed C columns at 30 °C running in (THF) at 1 $cm^3\ min^{-1}$ with a Roth Mocel 200 high precision pump. A DAWN DSP (Wyatt Technology) multiangle laser light scattering (MALLS) apparatus with 18 detectors and auxiliary Viscotek model 200 differential refractometer/viscometer detectors was used to calculate the molecular weights [referred to as gel permeation chromatography/light scattering (GPC/LS)].

1. Trans-[(Ph)(Et_3P)$_2$Pt–C≡C–R–C≡C–Pt(PEt_3)$_2$(Ph)] (R=carbazol-3,6-diyl) (M1)

A catalytic amount (~5 mg) of CuI was added to a stirred solution of *trans*-[$(PEt_3)_2$(Ph)PtCl] (0.543 g, 1.0 mmol) and 3,6-diethynylcarbazole (0.107 g, 0.5 mmol) in CH_2Cl_2/Pr_2NH (50 cm^3, 1:1 v/v) under nitrogen The yellow solution was stirred at room temperature for 15 h, after which all volatile components were removed under reduced pressure. The residue was dissolved in CH_2Cl_2 and passed through a silica column eluting with hexane/CH_2Cl_2 (1:1 v/v) giving compound M1 as a pale yellow solid in an isolated yield of 75% (0.46 g). IR (CH_2Cl_2): $\tilde{\nu}$ 2095 cm^{-1} (–C≡C–). ^{1}H NMR (250 MHz, $CDCl_3$): δ 7.53 (*d*, 2H, H-4,5), 7.41 (*d*, 2H, H-2,7), 7.32 (*dd*, 4H, H_{ortho} of Ph), 7.26 (*d*, 2H, H-1,8), 6.96 (*t*, 4H, H_{meta} of Ph), 6.80 (*t*, 2H, H_{para} of Ph), 9.55 (*s*, 1H, NH), 1.82–1.75 (*m*, 24H, PCH_2), 0.86 (*t*, 36H, CH_3). ^{13}C NMR (100 MHz, $CDCl_3$): δ 156.43 (C-10,13), 150.41 (C-11,12), 139.20–118.69 (C-1 to C-8 and Ph Cs), 112.73, 111.56 (–C≡C–), 14.95 (CH_2), 8.33 (CH_3). ^{31}P{^{1}H} NMR (101.3 MHz, $CDCl_3$): δ−131.17, $^1J_{Pt-P}$ =2643 Hz. FAB mass spectrum: m/z 1230.25 (M^+). Found: C, 50.99; H, 6.37. Calculated for $C_{52}H_{77}P_4Pt_2N$: C, 50.77; H, 6.31%.

2. Trans-[(Ph)(Et_3P)$_2$Pt–C≡C–R–C≡C–Pt(PEt_3)$_2$(Ph)] (R=carbazole-2,7-diyl) (M2)

Similar procedures were adopted as described above for M1 using 2,7-diethynylcarbazole instead of 3,6-diethynylcarbazole giving a pale yellow solid in 75% yield. IR (CH_2Cl_2): $\tilde{\nu}$ 2091 cm^{-1} (–C≡C–). ^{1}H NMR (250 MHz, $CDCl_3$): 7.55 (*d*, 4H, H_{ortho} of Ph), δ 7.36 (*d*, 2H, H-4,5), 7.30 (*s*, 2H, H-1,8), 7.17 (*dd*, 2H, C-3,6), 6.98 (*t*, 4H, H_{meta} of Ph), 6.82 (*t*, 2H, H_{para} of Ph), 9.60 (*s*, 1H, NH), 1.80 (*m*, 24H, PCH_2), 1.12 (*m*, 36H; CH_3). ^{13}C NMR (100 MHz, $CDCl_3$): δ 140.4 (C-10, 13), 139.4 (C-11,12), 127.7–119.6 (C-1 to C-8 and Ph Cs), 112.6 (–C≡C–), 14.77 (CH_2), 8.10 (CH_3). ^{31}P{^{1}H} NMR (101.3 MHz, $CDCl_3$): δ−131.85, $^1J_{Pt-P}$=2634 Hz. FAB mass spectrum: m/z 1230.25 (M^+). Found: C, 50.89; H, 6.35%. Calculated for $C_{52}H_{77}P_4Pt_2N$: C, 50.77; H, 6.31.

3. Trans-[(Ph)(Et_3P)$_2$Pt–C≡C–R–C≡C–Pt(PEt_3)$_2$(Ph)] (R=N-(2-ethyl-hexyl) carbazole-2,7-diyl) (M3)

This compound was obtained as a pale yellow solid in 78% yield by adopting similar procedures as described above using *N*-octyl-2,7-diethynylcarbazole. IR (CH_2Cl_2): $\tilde{\nu}$ 2090 cm^{-1} (–C≡C–). ^{1}H NMR (250 MHz, $CDCl_3$): δ 7.81 (*d*, 2H, H-4,5), 7.35 (*d*, 4H, H_{ortho} of Ph), 7.25 (*s*, 2H, C-1,8), 7.14 (*dd*, 2H, H-3,6), 6.97 (*t*, 4H, H_{meta} of Ph), 6.88 (*t*, 2H, H_{para} of Ph), 4.05 (*m*, 2H, NCH_2), 1.81 (*m*, 24H, PCH_2), 1.57 (*m*, 1H, CH alkyl), 1.38 (*m*, 8H, CH_2 alkyl), 1.14 (*m*, 36H, CH_3, of PEt_3), 0.88 (*t*, 6H, CH_3 alkyl). ^{13}C NMR (100 MHz, $CDCl_3$): δ 176.9 (C-10,13), 141.8, 139.7 (C-11,12), 127.7–119.5 (C-1 to C-8 and Ph Cs), 112.1, 111.2 (–C≡C–), 47.6–15.4 (CH_2 in C_8H_{17} and Et_3P), 14.4–11.2 (CH_3 in C_8H_{17}), 8.4 (CH_3 in Et_3P). ^{31}P{^{1}H} NMR (101.3 MHz, $CDCl_3$): δ−131.8, $^1J_{Pt-P}$=2630 Hz. FAB mass spectrum: m/z 1342.10 (M^+). Calculated for $C_{80}H_{93}P_4Pt_2N$: C, 53.69; H, 6.98. Found: C, 53.72; H, 6.91%.

4. Trans-[–(Bu_3P)$_2$Pt–C≡C–R–C≡C–]$_n$ (R=carbazol-3,6-diyl) (P1)

CuI (~5 mg) was added to a mixture of *trans*-[$Pt(P^nBu_3)_2Cl_2$] (0.670 g, 1.0 mmol) and 3,6-diethynylcarbazole (0.215 g, 1.0 mmol) in $^iPr_2NH$/CH_2Cl_2 (50 cm^3, 1:1 v/v). The solution was stirred at room temperature for 15 h, after which all volatile components were removed under reduced pressure. The residue was dissolved in CH_2Cl_2 and passed through a short alumina column. After removal of the solvent by a rotary evaporator, an off-white film was obtained readily which was then washed with methanol to give the polymer P1 in 70% isolated yield. Further purification can be accomplished by precipitating the polymer solution in dichloromethane from methanol. IR (CH_2Cl_2): $\tilde{\nu}$ 2095 cm^{-1} (–C≡C–). ^{1}H NMR (250 MHz, $CDCl_3$): δ 7.50 (*d*, 2H, H-4-5), 7.41 (*dd*, 2H, H-1,8), 7.25 (*d*, 2H, H-2,7), 9.57 (*s*, 1H, NH), 2.20–2.01 (*m*, 12H, PCH_2), 1.67–1.01 (*m*, 24H, CH_2), 0.93 (*t*, 18H, CH_3). ^{13}C NMR (100 MHz, $CDCl_3$): δ 150.28 (C-10, 13), 137.89 (C-11, 12), 129.56–118.76 (C-1 to C-8), 112.23, 111.16 (–C≡C–), 15.01 (CH_2), 9.77 (CH_3). ^{31}P{^{1}H} NMR (101.3 MHz, $CDCl_3$): δ −138.03, $^1J_{Pt-P}$=2363 Hz. Calculated for $[C_{40}H_{61}P_2NPt]_n$: C, 59.10; H, 7.56. Found: C, 59.26; H, 7.51%. M_n =17 900 g mol^{-1} (n=22), M_w=30 500 g mol^{-1}, polydispersity index (PDI)=1.7.

5. Trans-[(Bu_3P)$_2$Pt–C≡C–R–C≡C–]$_n$ (R=carbazole-2,7-diyl) (P2)

This compound was synthesized by adopting similar procedures as described above for P1 using (*trans*-[$(PBu_3)_2PtCl_2$]) and 2,7-diethynylcarbazole and a brown film was obtained in 70% yield. IR (CH_2Cl_2): $\tilde{\nu}$ 2095 cm^{-1} (–C≡C–). ^{1}H NMR (250 MHz, $CDCl_3$): δ 7.81 (*dd*, 2H, C-4,5), 7.27 (*s*, 2H, C-1,8), 7.15 (*d*, 2H, C-3,6), 9.65 (*s*, 1H, NH), 2.18 (*m*, 12H, PCH_2), 1.58 (*m*, 12H, CH_2), 1.30 (*m*, 12H, CH_2), 0.90 (*m*, 18H, CH_3). ^{13}C NMR (100 MHz, $CDCl_3$): δ 140.0 (C-10, 13), 127.6 (C-11,12), 119.8 (C-1,8), 101.2 (–C≡C–), 15.77 (CH_2), 9.98 (CH_3). ^{31}P{^{1}H} NMR (101.3 MHz, $CDCl_3$): δ−137.5, $^1J_{Pt-P}$=2339 Hz. Calculated for $[C_{40}H_{61}P_2PtN]_n$: C, 59.10; H, 7.56. Found: C, 59.25; H, 7.49%. GPC (THF): M_n=25 500 g mol^{-1} (n=31), M_w =40 500 g mol^{-1}, PDI=1.6.

6. Trans-[–(Bu_3P)$_2$Pt–C≡C–R–C≡C–]$_n$ (R=N-(2-ethylhexyl)carbazole-2,7-diyl) (P3)

This compound was synthesized by adopting similar procedures as described above for P1. Brown solid (72%yield). IR (CH_2Cl_2): $\tilde{\nu}$ 2094 cm^{-1} (–C≡C–). ^{1}H NMR (250 MHz, $CDCl_3$): δ 7.83 (*d*, 2H, H-4-5), 7.21 (*s*, 2H, H-1,8), 6.99 (*d*, 2H, H-3,6), 4.04 (*m*, 2H, NCH_2), 1.57 (*m*, 1H, CH alkyl), 2.22 (*m*, 12H, PCH_2), 1.52 (*m*, 32H, CH_2), 0.95 (*m*, 24H, CH_3). ^{13}C NMR (100 MHz, $CDCl_3$): δ 141.41 (C-10,13), 133.52 (C-11,12), 122.56-119.18 (C-1 to 8), 110.80 (–C≡C–), 47.59 (PCH_2), 39.21–17.23 (CH_2), 8.87

TABLE I. Synthetic and other characterization data for M1–M3 and P1-P3.

Compound	Yield	M_w	M_n	n	$\tilde{\nu}_{C\equiv C}$ (cm^{-1})	$^{31}P\{^1H\}$ NMR (ppm)[a]
M1	75	1 230.2	⋯	⋯	2095	−131.17 ($^1J_{Pt-P}$=2630 Hz)
M2	58	1 230.2	⋯	⋯	2091	−131.85 ($^1J_{Pt-P}$=2630 Hz)
M3	78	1 342.1	⋯	⋯	2090	−131.80 ($^1J_{Pt-P}$=2630 Hz)
P1	70	30 500	17 900	22	2095	−138.03 ($^1J_{Pt-P}$=2331 Hz)
P2	70	40 500	25 500	31	2095	−137.50 ($^1J_{Pt-P}$=2339 Hz)
P3	72	72 000	40 000	43	2094	−137.55 ($^1J_{Pt-P}$=2335 Hz)

[a]Referenced to $(MeO)_2P$.

(CH_3). $^{31}P\{^1H\}$ NMR (101.3 MHz, $CDCl_3$): δ−137.55, $^1J_{Pt-P}$=2335 Hz. Calculated for $[C_{48}H_{77}P_2PtN]_n$: C, 62.31; H, 8.39. Found: C, 62.20; H, 8.36%. GPC (THF): M_n =40 000 g mol^{-1} (n=43), M_w=72 000 g mol^{-1}, PDI= =1.8. [Fig. 1(b), Table I]

B. Optical measurements

Solutions of the materials were prepared at a concentration of typically 10–20 mg/ml in dichloromethane. Films of the materials with thicknesses of 100–150 nm were obtained by spin coating onto quartz. Absorption spectra were taken using a Hewlett-Packard ultraviolet-visible (UV-VIS) absorption spectrometer. For both photoluminescence (PL) and photoinduced absorption (PA) spectra, samples were mounted in a continuous flow helium cryostat where the temperature was controlled with an Oxford Intelligent temperature controller 4 (ITC-4). For low temperature emission spectral measurements of the M1 and P1, the 325 nm line of a He–Cd laser was used as excitation source. The room temperature photoluminescence of M1 and P1 was measured using a Cary Eclipse spectrofluorimeter from Varian. For the rest of the measurements, excitation was provided both by the UV lines (355–364 nm) of a continuous wave Ar^+ laser with typical intensities of a few mW/mm^2. PL spectra were recorded using a spectrograph with an optical fiber input coupled to a cooled charge coupled device (Oriel Intraspec IV). For photoinduced absorptions measurements, monochromated light from a 150 W tungsten-halogen lamp was used as the probe beam. The transmitted beam was dispersed through a second monochromator (both monochromators are Chromex SM250) and detected with a Si photodiode connected to a SR830 lock-in amplifier. The pump beam provided by the laser was chopped at 125 Hz. Frequencies of 4 Hz–3.5 kHz were used to measure the frequency dependence of the induced absorption.

III. RESULTS

A. Synthesis

The CuI-catalyzed polycondensation reaction between *trans*-$[(P^nBu_3)_2PtCl_2]$ and the terminal dialkynes (1:1 equivalent) in CH_2Cl_2/Pr_2NH readily provided the poly-ynes P1–P3. The dehydrohalogenation reaction of *trans*-$[(Ph)\times(Et_3P)_2PtCl]$ with half equivalent of the terminal dialkynes under similar conditions gave the Pt(II) diynes M1–M3. The synthesis scheme of the platinum(II) diynes and poly-yne is outlined in Fig. 1(b). Purification of Pt(II) diynes was accomplished by silica column chromatography while the Pt(II) poly-ynes were purified by chromatography on an alumina column.

B. Spectroscopic characterization

Systematic characterization of the Pt(II) diynes and poly-ynes was achieved by spectroscopic methods (IR, ^1H, ^{13}C, and ^{31}P NMR). The IR spectra of the diynes and poly-ynes provided clear evidence for the presence of the C≡C bond in the compounds, detected by its typical absorption at 2095 cm^{-1}. The single, sharp $\tilde{\nu}_{C\equiv C}$ absorption band indicates a *trans*-configuration of the ethynyl ligands around Pt(II)-phosphine moieties. The ^1H and ^{13}C NMR spectra of all the compounds showed the expected peaks corresponding to the alkyl, aryl, and alkynyl fragments. The ^{31}P NMR spectra displayed a signal at around −131 and −138 ppm for the diynes and poly-ynes, respectively, confirming the *trans*-configuration of the phosphines. The spectral features are similar to other Pt(II) diynes and poly-ynes previously reported[27–30] and confirm the all-*trans* configuration of the Pt(II) di- and poly-ynes. Gel permeation chromatography using a polystyrene (PS) calibration shows that the number-average molecular weights of the poly-ynes are in the range of 18 000–40 000 g/mol, corresponding to degrees of polymerization (n) between 22 and 43. The molecular weights should be viewed with caution bearing in mind the difficulties associated with utilizing GPC for rigid-rod polymers. GPC does not give absolute values of molecular weights but provides a measure of hydrodynamic volume. Rodlike polymers in solution possess very different hydrodynamic properties than flexible polymers. Therefore, calibration of the GPC with PS standards is likely to inflate the values of the molecular weights of the poly-ynes to some extent. However, the lack of discernable resonances that could be attributed to end groups in the NMR spectra provides support for the view that there is high degree of polymerization in these poly-ynes.

C. Absorption

Optical absorption spectra of the polymers and corresponding monomers were taken at room temperature in thin films and are shown in Fig. 2. The S_0-S_1 absorption band occurs between 3 and 4 eV and is associated with a transition that usually has a strong contribution from the $\pi-\pi^*$ transition of the conjugated ligand.[23,29,31] For the *para*-linked systems, the dominant absorption bands of the polymers are lowered with respect to those of the corresponding mono-

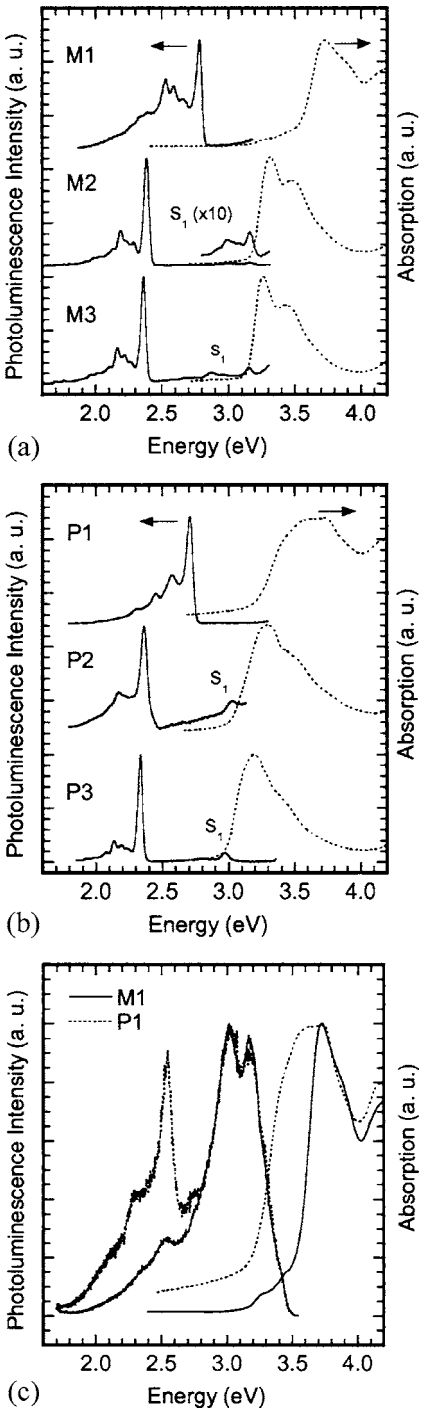

FIG. 2. Room temperature optical absorption (dotted line) and photoluminescence (PL) spectrum at 10 K (solid line) of (a) M1, M2, and M3 and (b) P1, P2, and P3. (c) Room temperature PL and absorption of M1 (solid line) and P1 (dotted line).

mers, indicating that the corresponding optical absorption transition in the polymers arises from an electronic excitation that is delocalized over more than one monomer unit.[12,13,29,32–36] The first absorption band of the *meta*-linked compounds is more complex and is compared in Fig. 2(c). The monomer M1 has a strong peak at 3.73 eV (332 nm) and two weak shoulders at 3.43 eV (362 nm) and 3.24 eV (383 nm). In the polymer, these features are broadened into a wide band centered at about 3.6 eV. The same features are reported yet not commented upon by Wong *et al.*[23] for $[Pt-T(C_4H_9-C)T]_1$, that is, a compound identical to M1 except that the H at the 9 position in M1 is replaced by a butyl group. In order to clarify the origin of the two low intensity shoulders, we took absorption measurements in solution at concentrations of 0.25 mg/ml, once in the highly polar solvent acetonitrile and once in the nonpolar solvent cyclohexane. In solution, we observe firstly the same intensity distribution between the peak and the shoulders as in the film and secondly a small overall hypsochromic shift with respect to the film (3.77, 4.48, and 3.30 eV, i.e., 329, 356, and 376 nm, for the peak and the two shoulders). However, we observe no difference in the spectral positions of the shoulders between the polar and the nonpolar solvent other than some overall broadening in acetonitrile, so that the two shoulders are unlikely to be charge transfer transitions. In the polymer P1, the two shoulders have gained intensity and have merged with the peak at 3.7 eV into a broadband. It therefore appears that the low intensity of the two shoulders may be caused by some symmetry-based selection rules that no longer apply in the polymer.

D. Photoluminescence

In the emission spectra obtained at 10 K [Figs. 2(a) and 2(b)], we observe two bands for the *para*-linked compounds, a weak higher energy one around 3 eV and an intense lower energy one at about 2.35 eV. We attribute the weak high energy feature in P2 and P3 to $S_1 \rightarrow S_0$ fluorescence due to the small energy shift between the bands in the absorption and the emission spectra. For M2 and M3, singlet emission can be observed at around 3.15 eV. The intense feature at about 2.35 eV for P2, P3, M2, and M3 is typical for $T_1 \rightarrow S_0$ phosphorescence in these Pt-containing conjugated polymers;[12,29,37] it has a long lifetime of about 160 μs (in M3, see below), has a strong temperature dependence in the polymer (not shown here), shows a strong vibronic structure which excludes an excimer origin,[28,38] and is located about 0.7 eV below the singlet emission, which is characteristic for T_1 emission in such *para*-linked rigid-rod polymers.[12,29,37,38]

For the *meta*-linked compounds at 10 K, we observe only one peak at 2.71 eV in P1 and 2.78 eV in M1. Due to the large energy shift from the peak of the singlet absorption and the strong vibronic structure, we also attributed this peak to a $T_1 \rightarrow S_0$ transition. No singlet emission can be observed at 10 K due to the strong phosphorescence background and the close proximity of the exciting laser line (at 3.5 eV) to the expected energy of the singlet emission. At room temperature the intensity of the triplet state emission is greatly reduced because of thermally activated diffusion to quenching sites. Furthermore, it is possible to use a spectrofluorimeter with excitation at 3.9 eV. Consequently, it is possible to observe the singlet emission band in M1 and P1 with two peaks at about 3.0 and 3.18 eV [Fig. 2(c)]. Our results compare well with a report by Wong *et al.* which investigates a polymer and monomer with the same structure as M1 and P1 except that the hydrogen at the carbazole nitrogen atom is replaced by a butyl group.[30] Wong *et al.* observe the peaks of the singlet emission at about 2.9 and 3.1 eV and the phosphorescence at about 2.7 eV. They study the temperature de-

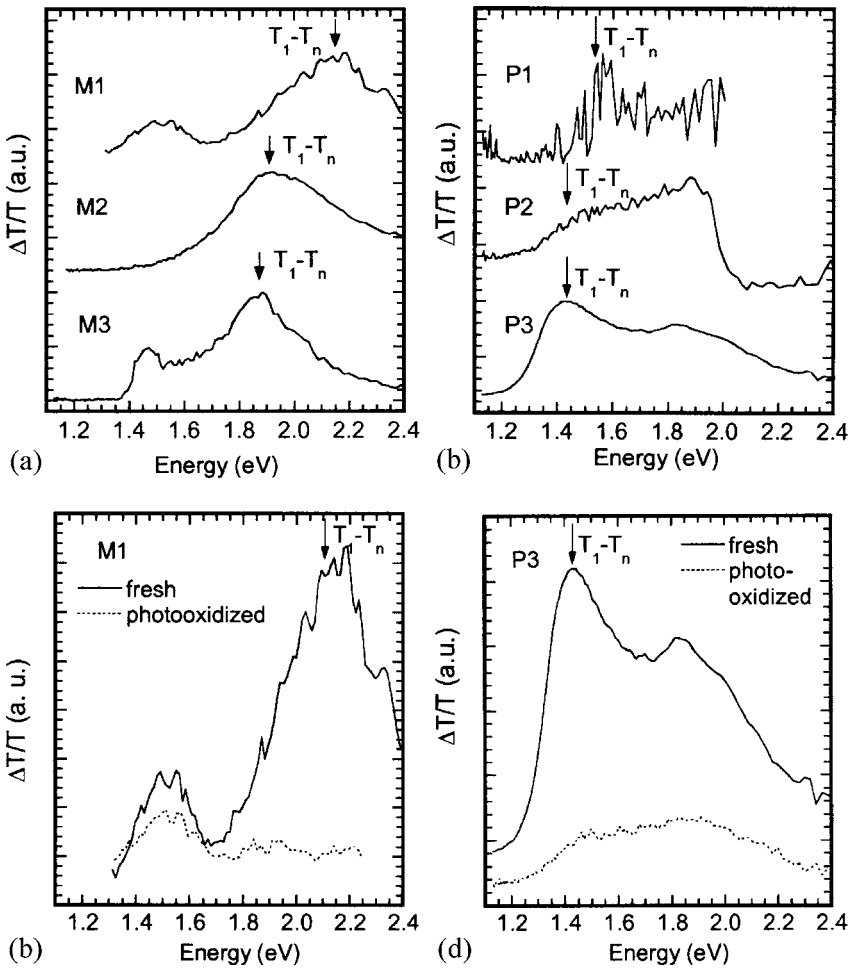

FIG. 3. (a) Photoinduced absorption at 10 K of M1, M2, and M3. (b) Comparison of the photoinduced absorption at 10 K of M1 in a fresh and a photo-oxidized film. (c) Photoinduced absorption at 10 K of P1, P2, and P3. (d) Comparison of the photoinduced absorption at 10 K of P3 in a fresh film and a photo-oxidized film.

pendence of the emission and hardly find any change in peak position for the singlet which justifies the use of the room temperature singlet energies we obtained for M1 and P1 for comparison against the 10 K singlet energies for the *para*-linked compounds. As observed earlier by Wong *et al.*, there is a strong dependence of the relative intensity distribution within the phosphorescence band such that the highest energy peak reduces strongly with increasing temperature.

E. Photoinduced absorption

In order to further access the triplet manifold, we have measured the T_1-T_n photoinduced absorption (Fig. 3). For the monomers, we observe a strong peak centered at about 2.1 eV (M1) and 1.9 eV (M2, M3). In M1 and M3, a smaller low energy peak is also detected at 1.5 and 1.45 eV, respectively. In order to unambiguously assign the $T_1 \rightarrow T_n$ transition, we measured the dependence of the photoinduced absorption and photoluminescence signal on the modulation frequency for M3 (Fig. 4) below. This gives a measure for the lifetime of the triplet state from which the absorption and emission occur. We fitted the data according to the monomolecular decay equation:[39]

$$S(\omega,\tau) = \frac{A\tau}{\sqrt{1+\omega^2\tau^2}},$$

where $S(\omega,\tau)$ is the magnitude of the signal, A is a constant, and τ is the lifetime of a single species.

The $T_1 \rightarrow S_0$ photoluminescence (PL) at 2.36 eV and the photoinduced absorption (PA) signal at 1.88 eV show a very similar frequency dependence with lifetimes of 160±30 and 110±30 μs, respectively. In contrast, the frequency dependence of the photoinduced absorption signal at 1.45 eV is very noisy, yet still distinctly different from that of the phosphorescence signal. We therefore assign the feature at around 1.88 eV to the $T_1 \rightarrow T_n$ transition. For M1, the photoinduced absorption signal is too low to measure a frequency depen-

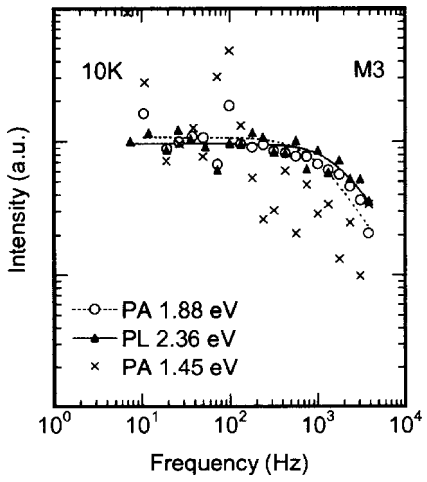

FIG. 4. Frequency dependence of the photoinduced absorption at 10 K of M3.

dence. In analogy to M3, we associate the high energy feature centered at 2.1 eV with the triplet state, while the low energy feature at 1.5 eV may be of a different electronic origin such as a bipolaron or an interchain absorption. This assignment is also verified by the effect of photo-oxidation on the PA spectrum of M1 [Fig. 3(b)]; the high energy peak associated with the T_1-T_n transition is fully quenched upon photo-oxidation, while the low energy peak persists. These values are in good agreement with results found on related monomers where the T_1-T_n energies range around 2.0–2.2 eV.[32,37]

In the polymers, the T_1-T_n transitions occur at lower energies, as observed earlier.[32,37] For the *para*-linked systems P2 and P3, the polymer PA spectra show two broad peaks at ~1.9 and ~1.5 eV. We assign the high energy PA peak to the charge separated state and the low energy peak around 1.5 eV to the triplet state T_1-T_n transition. This assignment is supported by the spectrum taken on photo-oxidized films of P3 [Fig. 3(d)] where the low energy peak is strongly quenched and the high energy peak gains much more importance.

IV. DISCUSSION

The fabrication of efficient phosphorescent light-emitting diodes requires host-guest systems where the singlet energy of the host is not too high such as to allow for good charge injection, while the host triplet energy level should be high enough to enable energy transfer from host to guest (or at least prevent transfer from guest to host). Recently it has been shown that carbazole can fulfill these requirements with S_1-T_1 energy gaps as low as 0.4 eV for both oligomers and polymers, provided that the units are connected at the *meta*-position.[17,18] This is in strong contrast to *para*-linked rigid-rod polymers such as poly(phenylenes), poly(phenylene-vinylenes), and poly(phenylene-ethynylenes), where the exchange energy is usually about 0.7 ± 0.1 eV for polymers and increases even further for oligomers.[12,13] Here we aim to understand the electronic origin of this stark difference in exchange energy that is observed for a *meta* versus a *para*-linkage. We use a monomer and a polymer with a carbazole unit connected via the *meta* or the *para* positions in order to asses the impact of π delocalization on the energy of the excited states in both cases.

The excited state energies derived from the spectroscopic results are summarized in Table II. The singlet and triplet energies are taken from the 0-0 position of the fluorescence and phosphorescence at 10 K, respectively, except for M1 and P1 where the room temperature fluorescence spectra are used. The energies of the T_n state are obtained by adding the energies of the $T_1 \rightarrow S_0$ and $T_1 \rightarrow T_n$ transitions. We briefly summarize the main results obtained from this table, which we will then discuss in the following.

(1) Comparison of *meta*- versus *para*-linkage in monomers. Considering first the monomers, we find that the S_1 state energies are identical in these two differently linked monomers while the energies of the T_1 and T_n states are lower in the *para*-linked monomer than in the *meta*-linked monomers. Consequently, the S_1-T_1 energy gap is about twice as large for the *para*-linkage than for the *meta*-linkage.

(2) Comparison of *meta*- versus *para*-linkage in polymers. Considering next the results on the polymers, the S_1, T_1, and T_n energies are lower for the *para*-linkage than for the *meta*-linkage. Similar to the monomer, the exchange energy is higher in the *para*-linked compound than in the *meta*-linked compound.

(3) Effect of polymerization on the *para*-linked compounds M2, P2 and M3, P3. The energies of the excited states are reduced, as is the exchange energy. This effect is strongest for T_n, strong for S_1, and weak for T_1 (with shifts of about 0.49, 0.14, and 0.02 eV, respectively, between M2 and P2).

(4) Effect of polymerization on the *meta*-linked compounds M1 and P1. The energy of the first excited states S_1 and T_1 hardly changes while the energy of the higher excited T_n state reduces by 0.65 eV.

TABLE II. (a) Energy levels for the monomers M1, M2, and M3. (b) Energy levels for the polymers P1, P2, and P3.

(a)	Monomer	M1 (eV)	M2 (eV)	M3 (eV)
	S_1	3.18	3.17	3.15
	T_1	2.78	2.39	2.36
	T_n	4.93	4.30	4.23
	S_1-T_1	0.40	0.78	0.79
	T_1-T_n	2.15	1.91	1.87
(b)	Polymer	P1 (eV)	P2 (eV)	P3 (eV)
	S_1	3.18	3.03	2.97
	T_1	2.71	2.37	2.33
	T_n	4.28	3.81	3.77
	S_1-T_1	0.47	0.66	0.64
	T_1-T_n	1.57	1.44	1.44

In order to understand the origin of these energy levels and, in particular, the small exchange energy in the *meta*-linked monomer, it is instructive to compare the pathway for conjugation for the *para*-linked compound and the *meta*-linked compound using the crude picture of resonance structures (Fig. 5). In the *para*-linked monomer M2, conjugation in the carbazole unit can occur via the phenyl rings without any involvement of the nitrogen. In that case, electron and hole are both delocalized along the π system, leading to a high degree of conjugation. This oversimplified picture is consistent with calculations based on density functional theory by Marsal *et al.*[40] that show large coefficients on the *para* position in HOMO and LUMO, provided that the carbazole is connected to a electron-donating moiety.

When the repeat units are polymerized, conjugation continues through the platinum atoms.[32,33,41] The excited states are no longer confined and their energies stabilize. This effect is particularly strong for the highly extended T_n state, strong for the extended S_1 state, and weak for the intrinsically less extended T_1 state. This particle-in-a-box effect has been observed before for other Pt-containing polymers.[13,32–38]

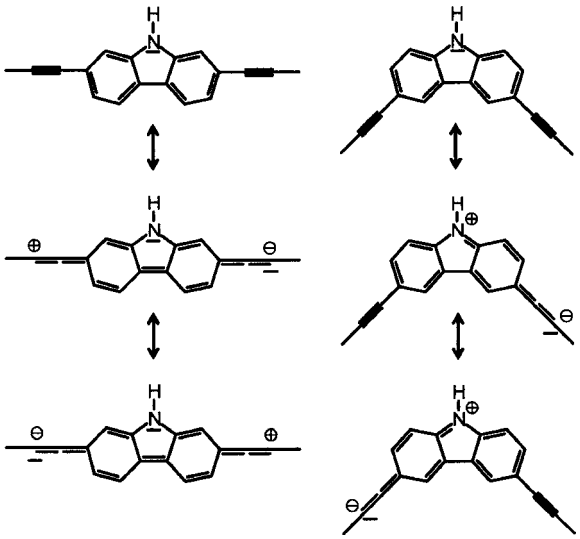

FIG. 5. Scheme of the resonance structures for a carbazole unit that is connected via the *para* (2,7) position (left) or the *meta* (3,6) position (right).

In contrast, in the *meta*-linked monomer M1, some conjugation is only possible under incorporation of the nitrogen atom,[40] where the hole tends to localize in an orbital with some nonbonding character (see Fig. 5). This also restrains the movement of the more delocalized electron and so pins down the entire exciton. This has two consequences: First, polymerization has no effect on such a localized state, so that the energies of the singlet excited state in the monomer M1 and the polymer P1 do not differ. Second, the wave function overlap between the hole (partially localized at the nitrogen site) and the electron (more delocalized over the π^* system) is small, resulting in an exchange energy in the range of 0.4–0.5 eV. This is considerably less than the exchange energy observed when electron and hole are both delocalized in π and π^* orbitals (as in the *para*-linked compounds), which is typically at about 0.7 eV for polymers and at higher values for monomers (since the confinement of electron and hole in monomers increases the electron-hole overlap).[13]

The energy shift of the T_n state between M1 and P1 is large and of similar magnitude as that between M2 and P2 or M3 and P3. We consider this point to a higher degree of delocalization in such a higher excited state.

V. CONCLUSION

Host materials for polymer light-emitting diodes need to have a singlet S_1 energy that is not too high such as to allow for charge injection yet they should have a triplet T_1 energy that is high enough to allow for energy transfer onto blue emitting phosphorescent dyes. This requirement cannot be fulfilled with conjugated rigid-rod polymers where electron and hole are both delocalized in π^* and π orbitals, since their large wave function overlap leads to an exchange energy in the order of 0.7 eV and may be even higher for shorter oligomers or polymer backbones with some torsion.[12,13] We have demonstrated here that a small exchange energy on the order of 0.4–0.5 eV can be achieved in carbazole-containing polymers and monomers that are connected at the 3,6 (*meta*) position instead of the 2,7 (*para*-) position. We attribute this to the fact that the *meta*-linkage partially localizes the hole on the nitrogen site so that electron-hole overlap is reduced compared to that in the *para*-linkage. This concept may present a model for the systematic design of host polymers.

ACKNOWLEDGMENTS

The authors thank R. H. Friend and C. Dosche for helpful discussions. One of the authors (N.Z.) thanks the Gates Cambridge Trust and ORS for support. This work is supported by IG/SCI/CHEM/05/02.

[1] J. H. Burroughes, D. D. C. Bradley, A. R. Brown, R. N. Marks, K. McKay, R. H. Friend, P. L. Burn, and A. B. Holmes, Nature (London) **347**, 539 (1990).
[2] P. L. Burn, D. D. C. Bradley, A. R. Brown, R. N. Marks, K. McKay, R. H. Friend, and A. Kraft, J. Chem. Soc., Perkin Trans. 1 **1**, 3225 (1992).
[3] D. Braun and A. J. Heeger, Appl. Phys. Lett. **58**, 1982 (1991).
[4] C. Yang, Z. V. Vardeny, A. Köhler, M. Wohlgenannt, M. Al-Suti, and M. Khan, Phys. Rev. B **70**, 241202 (2004).
[5] M. Wohlgenannt and Z. V. Vardeny, J. Phys.: Condens. Matter **15**, R83 (2003).
[6] A. Köhler and J. S. Wilson, Org. Electron. **4**, 179 (2003).
[7] M. A. Baldo, S. Lamansky, P. E. Burrows, M. E. Thompson, and S. R. Forrest, Appl. Phys. Lett. **75**, 4 (1999).
[8] J. S. Wilson, A. S. Dhoot, A. J. A. B. Seeley, M. S. Khan, A. Köhler, and R. H. Friend, Nature (London) **413**, 828 (2001).
[9] M. Wohlgenannt, X. M. Jiang, Z. V. Vardeny, and R. A. J. Janssen, Phys. Rev. Lett. **88**, 197401 (2002).
[10] C. Adachi, M. A. Baldo, S. R. Forrest, S. Lamansky, M. E. Thompson, and R. C. Kwong, Appl. Phys. Lett. **78**, 1622 (2001).
[11] C. Adachi, M. A. Baldo, M. E. Thompson, and S. R. Forrest, J. Appl. Phys. **90**, 5048 (2001).
[12] A. Köhler, J. S. Wilson, R. H. Friend, M. K. Al-Suti, M. S. Khan, and A. Gerhard, H. Bassler, J. Chem. Phys. **116**, 9457 (2002).
[13] A. Köhler and D. Beljonne, Adv. Funct. Mater. **14**, 11 (2004).
[14] M. J. Yang and T. Tsutsui, Jpn. J. Appl. Phys., Part 2 **39**, L828 (2000).
[15] Y. Kawamura, S. Yanagida, and S. R. Forrest, J. Appl. Phys. **92**, 87 (2002).
[16] H. J. Changa, N. Y. Haa, A. Kima, J. Lima, B. Parka, E. J. Parkb, J. H. Imb, J. H. Kimb, S. H. Leeb, and J. W. Wu, Opt. Mater. (Amsterdam, Neth.) **21**, 413 (2002).
[17] A. V. Dijken, J. J. A. M. Bastiaansen, N. M. M. Kiggen, B. M. W. Langeveld, C. Rothe, A. Monkman, I. Bach, P. Stössel, and K. Brunner, J. Am. Chem. Soc. **126**, 7718 (2004).
[18] K. Brunner, A. V. Dijken, H. Börner, J. J. A. M. Bastiaansen, N. M. M. Kiggen, and B. M. W. Langeveld, J. Am. Chem. Soc. **126**, 6035 (2004).
[19] I. Avilov, P. Marsal, J. Bredas, and D. Beljonne, Adv. Mater. (Weinheim, Ger.) **16**, 1624 (2004).
[20] W. L. F. Armarego, D. D. Perrin, *Purification of Laboratory Chemicals*, 4th ed. (Butterworth-Heinemann, Guildford, UK, 1996).
[21] J. Chatt and B. L. Shaw, J. Chem. Soc. **1960**, 4020; W. Muller, G. Schmidtberg, and H. Brune, Chem. Ber. **118**, 4653 (1985).
[22] J. Chatt and R. G. Hayter, J. Chem. Soc. Dalton Trans. **1961**, 896.
[23] W. Wong, G.-L. Lu, K.-H. Choi, and J.-X. Shi, Macromolecules **35**, 3506 (2002).
[24] C. Beginn, J. V. Grazulevicius, and P. Strohriegl, Macromol. Chem. Phys. **195**, 2353 (1994).
[25] J. Bouchard, M. Belletete, G. Durocher, and M. Leclerc, Macromolecules **36**, 4624 (2003).
[26] For GPC procedural details, see *Organometallic Polymers*, edited by S. Takahasi, M. Kariya, T. Tatake, K. Sonogashira, and C. U. Pittman, Jr. (Academic, New York, 1978).
[27] M. S. Khan, A. K. Kakkar, N. J. Long, J. Lewis, P. R. Raithby, P. Nguyen, T. B. Marder, F. Wittmann, and R. H. Friend, J. Mater. Chem. **4**, 1227 (1994).
[28] N. Chawdhury, A. Köhler, R. H. Friend, W. Y. Wong, J. Lewis, M. Younus, P. R. Raithby, T. C. Corcoran, M. R. A. Al-Mandhary, and M. S. Khan, J. Chem. Phys. **110**, 4963 (1999).
[29] J. S. Wilson, A. Köhler, R. H. Friend, M. K. Al-Suti, M. R. A. Al-Mandhary, M. S. Khan, and P. R. Raithby, J. Chem. Phys. **113**, 7627 (2000).

[30] W. Y. Wong, K. H. Choi, G. L. Lu, and J. X. Shi, Macromol. Rapid Commun. **22**, 461 (2001).
[31] M. Younus, A. Köhler, S. Cron, N. Chawdhury, M. Al-Mandhary, M. S. Khan, J. Lewis, N. Long, R. H. Friend, and P. R. Raithby, Angew. Chem., Int. Ed. **37**, 3036 (1998).
[32] D. Beljonne, H. F. Wittmann, A. Köhler, S. Graham, M. Younus, J. Lewis, P. R. Raithby, M. S. Khan, R. H. Friend, and J. L. Brédas, J. Chem. Phys. **105**, 3868 (1996).
[33] O. Lhost, J. M. Toussaint, J. L. Brédas, H. F. Wittmann, K. Fuhrmann, R. H. Friend, M. S. Khan, and J. Lewis, Synth. Met. **57**, 4525 (1993).
[34] J. E. Rogers, B. C. Hall, D. C. Hufnagle, J. E. Slagle, A. P. Ault, D. G. McLean, P. A. Fleitz, and T. M. Cooper, J. Chem. Phys. **122**, 214708 (2005).
[35] J. E. Rogers, T. M. Cooper, P. A. Fleitz, D. J. Glass, and D. G. McLean, J. Phys. Chem. A **106**, 10108 (2002).
[36] Y. Liu, S. Jiang, K. Glusac, D. H. Powell, D. F. Anderson, and K. S. Schanze, J. Am. Chem. Soc. **124**, 12412 (2002).
[37] N. Chawdhury, A. Köhler, R. H. Friend, M. Younus, N. J. Long, P. R. Raithby, and J. Lewis, Macromolecules **31**, 722 (1998).
[38] J. S. Wilson, N. Chawdhury, M. R. A. Al-Mandhary, M. Younus, M. S. Khan, P. R. Raithby, A. Köhler, and R. H. Friend, J. Am. Chem. Soc. **123**, 9412 (2001).
[39] G. Dellepiane, C. Cuniberti, D. Comoretto, G. F. Musso, G. Figari, A. Piaggi, and A. Borghesi, Phys. Rev. B **48**, 7850 (1993).
[40] P. Marsal, I. Avilov, D. A. da Silva Filho, J. L. Breda, and D. Beljonne, Chem. Phys. Lett. **392**, 521 (2004).
[41] F. Wittmann, R. H. Friend, M. S. Khan, and J. Lewis, J. Phys. Chem. **101**, 2693 (1994).